Molecular Therapy
Oncolytics
Original Article

AMERICAN SOCIETY of GENE & CELL THERAPY

Systemically Administered Sindbis Virus in Combination with Immune Checkpoint Blockade Induces Curative Anti-tumor Immunity

Iris Scherwitzl,[1,2] Alicia Hurtado,[1,2] Carolyn M. Pierce,[1] Sandra Vogt,[1] Christine Pampeno,[1] and Daniel Meruelo[1]

[1]Department of Pathology, NYU School of Medicine, New York, NY 10016, USA

Oncolytic viruses represent a promising form of cancer immunotherapy. We investigated the potential of Sindbis virus (SV) for the treatment of solid tumors expressing the human cancer testis antigen NYESO-1. NYESO-1 is an immunogenic antigen frequently expressed in numerous cancers, such as ovarian cancer. We show that SV expressing the tumor-associated antigen NYESO-1 (SV-NYESO1) acts as an immunostimulatory agent, inducing systemic and rapid lymphocyte activation, leading to a pro-inflammatory environment. SV-NYESO1 treatment combined with anti-programmed death 1 (anti-PD-1) markedly augmented the anti-tumor immunity in mice over the course of treatment, resulting in an avid systemic and intratumoral immune response. This response involved reduced presence of granulocytic myeloid-derived suppressor cells in tumors and an increase in the activation of splenic and tumor-infiltrating T cells. Combined therapy also induced enhanced cytotoxic activity of T cells against NYESO-1-expressing tumors. These results were in line with an observed inverse correlation between T cell activation and tumor growth. Finally, we show that combined therapy resulted in complete clearance of NYESO-1-expressing tumors *in vivo* and led to long-term protection against recurrences. These findings provide a rationale for clinical studies of SV-NYESO1 combined with immune checkpoint blockade anti-PD-1 to be used in the treatment of NYESO-1-expressing tumors.

INTRODUCTION

Cancer immunotherapy requires elicitation of an immune response that recognizes, targets, and eliminates cancer cells. Several methods, including immune checkpoint blockade, cancer vaccine, and chimeric antigen receptor T cell treatment, have already been approved for the treatment of some cancers.[1–4] Although these methods are very promising, benefits are often observed for only a minority of patients.[5,6] Oncolytic virus (OV) immunotherapy has emerged in the last decades as another therapeutic approach to treat cancer. In 2015, talimogene laherparepvec (T-Vec) became the first approved OV by the US Food and Drug Administration (FDA).[7] Many other OVs are now under investigation in advanced trials for liver, prostate, bladder, and other cancers, with some encouraging data.[8–10] The therapeutic efficacy of OVs is achieved by a combination of selective tumor cell killing and establishment of a local anti-tumor immune response, which can have a systemic effect.[7,11–14] Moreover, OVs can be genetically engineered for optimization of tumor selectivity and enhanced stimulation of the immune response. Recently, clinical investigation of OVs are more and more focused in the immunostimulatory properties of these viruses, and combinatorial studies with immune checkpoint blockade have emerged, showing promising results.[9,15,16]

Sindbis virus is a member of the *Alphavirus* genus and an OV with marked oncolytic activity.[17,18] A Sindbis virus vector (SV) has several advantages that make it a good candidate for cancer therapy. First, SV has a positive sense single-stranded RNA genome, rendering the vector safer than DNA-based OVs, as the vector cannot incorporate its genome into the host's DNA.[19] Furthermore, in humans, Sindbis infection is considered asymptomatic, though infrequently, it can lead to mild fever, rash, and arthralgia that resolves promptly and, more rarely,[20–22] prevalently in some DRB1*01-positive individuals, arthritic symptomology that can persist longer.[23,24] To further enhance its safety, SV was genetically modified to be replication defective by splitting its genome so the replicon and gene of interest are separated from the structural genes and the packaging signal deleted from the later genome strand.[25] Last, due to the fact that Sindbis is a blood-borne pathogen, it can be administrated systemically in the bloodstream facilitating the delivery of the drug.[18]

We previously demonstrated using a tumor model expressing β-galactosidase (LacZ), that SV—expressing the tumor-associated antigen (TAA) LacZ (SV-LacZ)—transiently delivered the TAA to lymph nodes (LNs) and elicited a diversified anti-tumor $CD8^+$ T cell response, resulting in complete tumor clearance in most of the mice.[26] Because LacZ is not normally expressed in mammalian cells, we next wanted to test the therapeutic efficacy of SV in a clinically relevant tumor model. Therefore, a tumor cell line expressing the human cancer testis antigen NYESO-1 was used. NYESO-1 is an advantageous clinical antigen for use in immunotherapy due to its lack

Received 21 April 2018; accepted 28 April 2018;
https://doi.org/10.1016/j.omto.2018.04.004.

[2]These authors contributed equally to this work.

Correspondence: Daniel Meruelo, Department of Pathology, NYU School of Medicine, 550 First Avenue, 5th Floor, MSB507, New York, New York 10016, USA.
E-mail: daniel.meruelo@nyumc.org

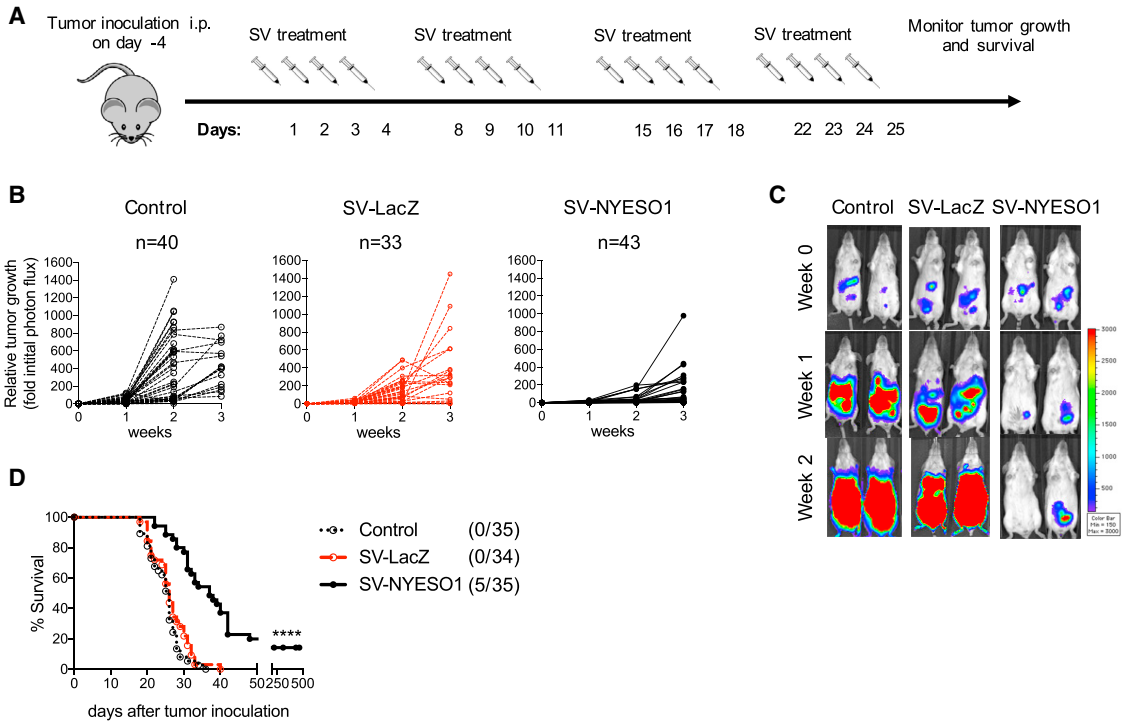

Figure 1. SVs Expressing the Tumor-Associated Antigen NYESO-1 Exhibit Enhanced Antitumor Efficacy *In Vivo*

(A) Treatment schema. BALB/c mice were injected i.p. (day −4) with CT26.Fluc.NYESO1 cells (7×10^4) on the right side of the abdomen. Five days later (day 1), SV-LacZ or SV-NYESO1 was injected into the left side of the abdomen for 4 consecutive days for a total of 4 weeks. Tumor growth was measured once a week using noninvasive bioluminescence imaging. (B) Tumor growth curves are shown as fold changes relative to the luminescence on day 0 of the same mouse. Left graph, no treatment (control, n = 40). Middle graph, treated with SV-LacZ (SV-LacZ, n = 33). Right graph, treated with SV-NYESO1 (SV-NYESO1, n = 43). (C) Representative bioluminescence images of control and SV-treated mice bearing CT26.Fluc.NYESO1 tumors. (D) Survival plots of untreated (Control, n = 35) and SV-NYESO1- (n = 35) or SV-LacZ (n = 34)-treated mice. Statistical significance between SV-LacZ and SV-NYESO1 was determined with the Mantel-Cox text. Results are representatives of at least two independent experiments. ****$p \leq 0.0001$.

of expression in tissues outside of the testes but frequent occurrence in numerous cancers, as well as its immunogenicity and its safety, which have been demonstrated in numerous clinical trials.[27] Presence of NYESO-1 is seen in approximately one-third to one-fourth of all melanoma, lung, esophageal, liver, gastric, prostate, ovarian, and bladder cancers. Although a rare cancer, over 80% of synovial sarcomas express NYESO-1.[28] Here, we examine the therapeutic efficacy of SV expressing the TAA NYESO-1 (SV-NYESO1) in immunocompetent mice. Our results demonstrate the importance of the addition of immune checkpoint blockade anti-programmed death 1 (anti-PD-1) to SV-NYESO1 therapy to induce a stronger systemic and intratumoral anti-tumor immune response that leads to total tumor clearance in the majority of treated animals as well as the rejection of tumor rechallenges. Thus, our treatment strategy could greatly improve the outcome of treatment for many NYESO-1-expressing tumors and merits consideration for clinical testing.

RESULTS

SVs Expressing the TAA NYESO-1 Exhibit Antitumor Efficacy *In Vivo*

To exploit the therapeutic effect of SV against human cancers, we genetically modified a replication-deficient SV to express the human cancer testis antigen NYESO-1 (SV-NYESO1; Figure S1A). NYESO-1 is an advantageous candidate for eliciting a tumor-specific immune response due to its restricted expression in normal tissues but frequent occurrence in numerous cancers, such as ovarian cancer, where it is expressed in 43% of cases.[27] To test SV-NYESO1 for cancer therapy, we intraperitoneally (i.p.) injected a tumor cell line expressing NYESO-1 and firefly luciferase (CT26.Fluc.NYESO1) into immuno-competent female mice. Expression of NYESO-1 by SV-NYESO1 and CT26.Fluc.NYESO1 was previously confirmed by western blot (Figures S1B and S1C). After the tumor had become established (4 days after tumor cell injection [day 0]), SV-NYESO1 was systemically injected on 4 consecutive days (days 1, 2, 3, and 4) for a total of 4 weeks (Figure 1A). To investigate the importance of the TAA NYESO-1 in the vector, SV expressing an unrelated antigen, β-galactosidase (LacZ), was used (Figures S1A and S1D). Tumor growth was measured once a week using noninvasive bioluminescent imaging (Figures 1B and 1C). Tumors grew progressively in both untreated animals (control) and mice treated with SV-LacZ. In contrast, systemically injected SV-NYESO1 induced a delay in tumor growth and in some cases resulted in complete regression. Tumor growth was inversely correlated with long-term survival, as all control and SV-LacZ-treated animals died after 3 weeks, and 15% to 20%,

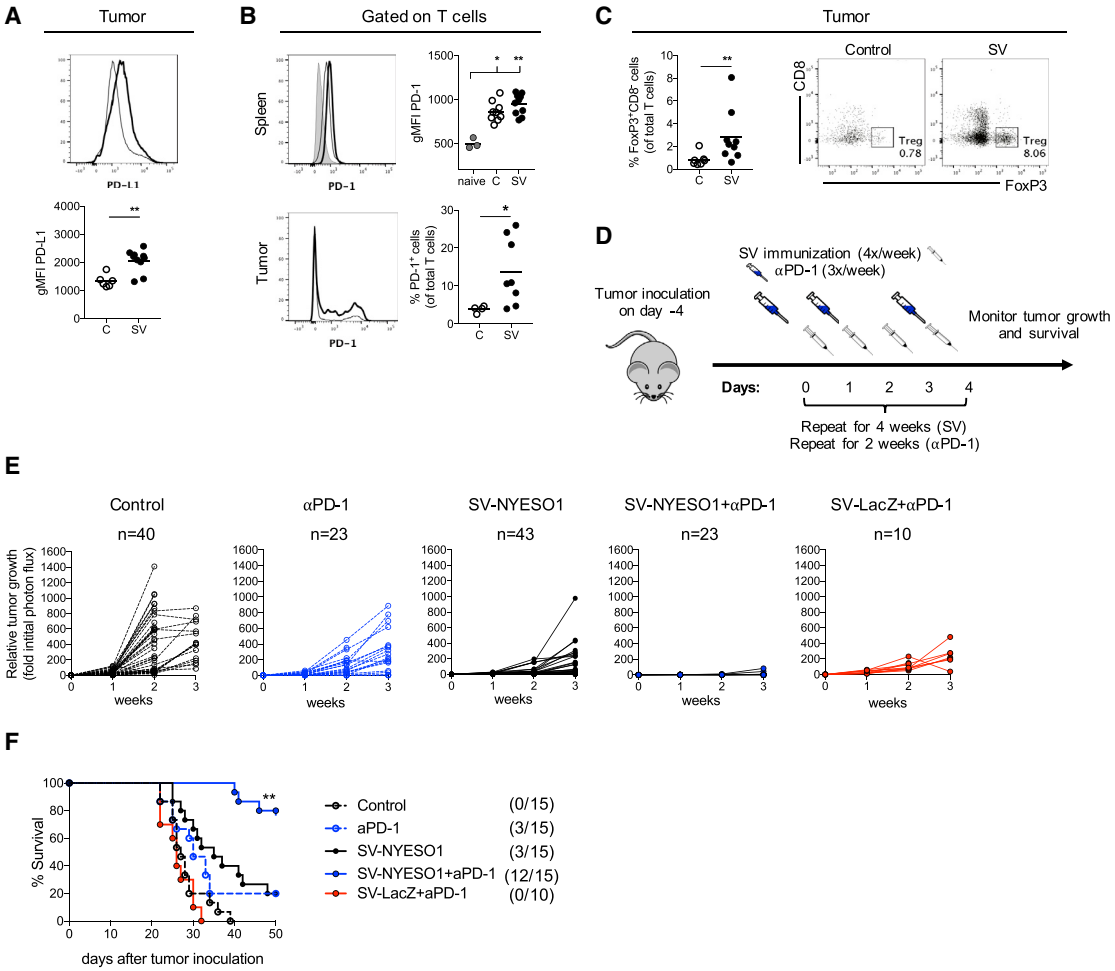

Figure 2. SV-NYESO1 in Combination with Anti-PD-1 Antibody Completely Inhibits Tumor Growth and Cures Mice from Established Tumors

(A) PD-L1 expression on the surface of tumor cells CT26.Fluc.NYESO1 *in vivo*. PD-L1 expression was analyzed by flow cytometry in untreated (C) and SV-NYESO (SV)-treated mice on day 14 and shown as histogram and bar graph. (B) PD-1 expression on T cells was analyzed by flow cytometry by gating on $CD3^+$ cells. Top graph, Splenocytes from naive (n = 3) and untreated (C, n = 9) or SV-NYESO1-treated (SV, n = 9) tumor-bearing mice on day 7. Bottom graph, T cells from tumor of untreated (C, n = 4) or SV-NYESO1-treated (SV, n = 8) tumor-bearing mice on day 14. Representative flow cytometry plots are shown as histograms. (C) Regulatory T cell frequency (T_{REG}) in tumor from control and SV-NYESO1-treated mice on day 14. Frequency was analyzed by flow cytometry, and results are shown as dot plots and bar graph. (D) Treatment schema used in (D) and (E). Tumor-bearing mice were left untreated or were treated with SV with or without anti-PD-1. (E) Tumor growth curves are shown as fold changes relative to the luminescence on day 0 of the same mouse. Left to right, untreated (control, n = 40), anti-PD-1 (αPD-1, n = 23), SV-NYESO1 (n = 43), SV-NYESO1 in combination with anti-PD-1 (SV-NYESO1 + αPD-1, n = 23), and SV-LacZ in combination with anti-PD-1 (SV-LacZ + αPD-1, n = 10)-treated mice. (F) Survival plots of untreated and treated mice. Statistical significance between SV-NYESO1 and SV-NYESO1 + αPD-1 was determined with the Mantel-Cox test. (A–C) Lines represent means, and statistical significance was determined with the Mann-Whitney test or with the Kurskal-Wallis test followed by the Dunns' test. (D and E) Results are representatives of at least two independent experiments. *$p < 0.05$, **$p \leq 0.01$.

depending on the experimental conditions, of the animals treated with SV-NYESO1 showed complete tumor clearance response (Figure 1D).

SV-NYESO1 in Combination with Anti-PD-1 Antibody Completely Inhibits Tumor Growth and Cures Mice from Established Tumors

Previous data from the lab demonstrated the crucial role of T cells in eradicating tumors in response to SV treatment.[26] In those studies, LacZ, a foreign antigen, was used, whereas in the current studies a cancer-testis-antigen is involved in the model. We postulated that SV-NYESO1 treatment may have been less efficacious due to the mitigation of the therapeutic activity of T cells by the tumor-specific expression of immune checkpoint molecule programmed death ligand 1 (PD-L1) as well as by the expression of programmed death protein 1 (PD-1) on T cells. Indeed, SV-NYESO1 therapy induced a significant increase of PD-L1 and PD-1 expression on tumor cells and tumor-infiltrating T cells, respectively (Figures 2A and 2B).

PD-1 expression on splenic T cells was similar in tumor-bearing mice with and without viral therapy (Figure 2B). In addition, an increase of regulatory T cells was observed in tumors from SV-NYESO1-treated mice when compared with control mice (Figure 2C). These observations suggest that SV-NYESO1 therapy may be augmented by anti-PD-1 treatment, as blockade of PD-1/PD-L1 reduces the number and/or suppressive activity of regulatory T cells and restores the activity of effector T cells.[29] To test this hypothesis, tumor-bearing mice were treated with SV-NYESO1 together with the checkpoint antibody anti-PD-1. Anti-PD-1 was injected three times a week (day 0, 2, and 4) for a total of 2 weeks (Figure 2D). The animals were then monitored for tumor growth once a week using noninvasive bioluminescent imaging (Figures 2E and S2). Again, tumors in untreated mice grew progressively and all mice succumbed to cancer after 3 weeks. SV-NYESO1 and anti-PD-1 alone induced a delay in tumor growth with moderate therapeutic efficacy of 15% to 20%, depending on the experimental condition. However, the combination of SV-NYESO1 and anti-PD-1 resulted in complete regression of tumors in almost all mice (12 of 15 mice) (Figure 2F). This effect was dependent on the expression of NYESO-1 by SV, as all mice (1 of 10 mice) treated with SV-LacZ and anti-PD-1 were unable to control tumor growth and succumbed to cancer. Thus, efficacy is dependent upon SV initially presenting the TAA present in the tumor; in this case NYESO-1 as well as the presence of the immune checkpoint blockade anti-PD-1.

SV-NYESO1 Acts as an Immunostimulatory Agent and Induces a Rapid and Systemic Lymphocyte Activation

Recently, it has become apparent that OVs can stimulate the immune response and trigger inflammation, which can enhance the anti-tumor response.[8] To analyze the effect of SV therapy on the immune response, the spleen, LNs, and plasma from all groups were collected on several days during treatment. First, the effect of one SV-NYESO1 injection on the immune response was investigated (Figure 3A). Plasma was collected on day 2 (24 and 48 hr after the first SV-NYESO1 and/or anti-PD-1 injection, respectively) and pro-inflammatory cytokines and chemokines were analyzed (Figure 3B). Pro-inflammatory cytokine levels of interferon-γ (IFN-γ), tumor necrosis factor α (TNF-α), and interleukin-2 (IL-2) showed a significant increase in SV-NYESO1-treated mice when compared with control and naive mice. The same trend was observed for chemokines CCL-2 and CCL-4, which have been shown to promote leukocyte recruitment to the site of inflammation and/or infection (Figure 3C; Castellino et al.[30]). No difference in cytokine and chemokines levels was detected between groups treated with SV-NYESO1 with and without anti-PD-1 (data not shown).

Next, we wondered whether the pro-inflammatory condition observed in the blood after one injection of SV-NYESO1 reflected the activation status of lymphocytes. Spleen and LNs were collected on day 2, and lymphocyte activation—as judged by the expression of the early activation marker CD69—was analyzed by flow cytometry. CD69 expression on $CD4^+$ and $CD8^+$ T cells (Figures 3D–3G) as well as on natural killer (NK) and B cells (Figure S3) was markedly upregulated in spleen, mediastinal, inguinal, and axillary LNs after one injection of SV-NYESO1 when compared with control mice and mice treated with anti-PD-1 alone. Even though a slight difference can be observed, there is no significant difference in T cell activation between mice treated with combined therapy and SV-NYESO-1-treated mice. Interestingly, the strongest lymphocyte activation was detected in mediastinal LN. This finding is consistent with published data from our lab demonstrating that SV quickly localizes in the mediastinal LN after i.p. injection.[26] In line with this observation, a strong T cell infiltration in mediastinal LN was observed in mice treated with SV-NYESO1 with and without anti-PD-1 (Figures 3H and 3I). These results demonstrate that replication-deficient SV-NYESO1 is a potent immunostimulatory agent, which quickly induces a systemic pro-inflammatory environment and lymphocyte activation.

Combined Therapy Enhances T Cell Activation and Function over the Course of Treatment

To better understand the role of anti-PD-1 in the combined therapy, T cell activation in peripheral lymphoid organs was determined over a 3-week period. After tumor inoculation (day −4), mice were treated with SV-NYESO1 four times a week (days 1, 2, 3, and 4) for a total of 4 weeks (Figure 4A). Anti-PD-1 antibody was administered to the respective groups three times a week (days 0, 2, and 4) for a total of 2 weeks. Spleen and LNs were collected on days 7, 14, and 21, and T cell activation was determined by assaying the expression of the activation and proliferation marker CD44 and Ki-67, respectively. CD44 and Ki-67 expression were substantially and continuously upregulated on splenic $CD4^+$ and $CD8^+$ T cells in animals treated with combined therapy when compared with SV-NYESO1 alone (Figures 4B and 4C). T cell activation was not observed in LNs, except for a slight increase in mediastinal LNs on day 14 (Figures S4A and S4B). In contrast to mice receiving SV-NYESO1 therapy, control mice and mice treated with anti-PD-1 alone showed no significant difference in T cell activation when compared with naive mice. Furthermore, a highly significant negative correlation between splenic T cell activation— as judged by CD44 and Ki-67 expression— and tumor growth was observed, suggesting that T cells have an important role in controlling tumor growth (Figures 4D and S4C). In line with these results, ELISPOT analysis of IFN-γ by splenocytes revealed that combined therapy accelerated and augmented IFN-γ secretion compared with SV-NYESO1 alone, with peak IFN-γ secretion on day 14 (Figure 4E). Splenocytes from mice treated with SV-NYESO1 alone produced a constant low level of IFN-γ over the course of treatment.

Having observed enhanced T cell activation and cytokine production in mice treated with combined therapy, the function of T cells was investigated using an *ex vivo* cytotoxic assay. Splenocytes obtained from all groups were co-cultured at various effector-to-target (E/T) cell ratios with the tumor cell line CT26.Fluc expressing the TAA NYESO-1 (CT26.NYESO1) or an unrelated antigen, LacZ (CT26.LacZ) (Figure 4E). The cytotoxic potential of splenocytes was determined by measuring the luciferase activity of CT26, which

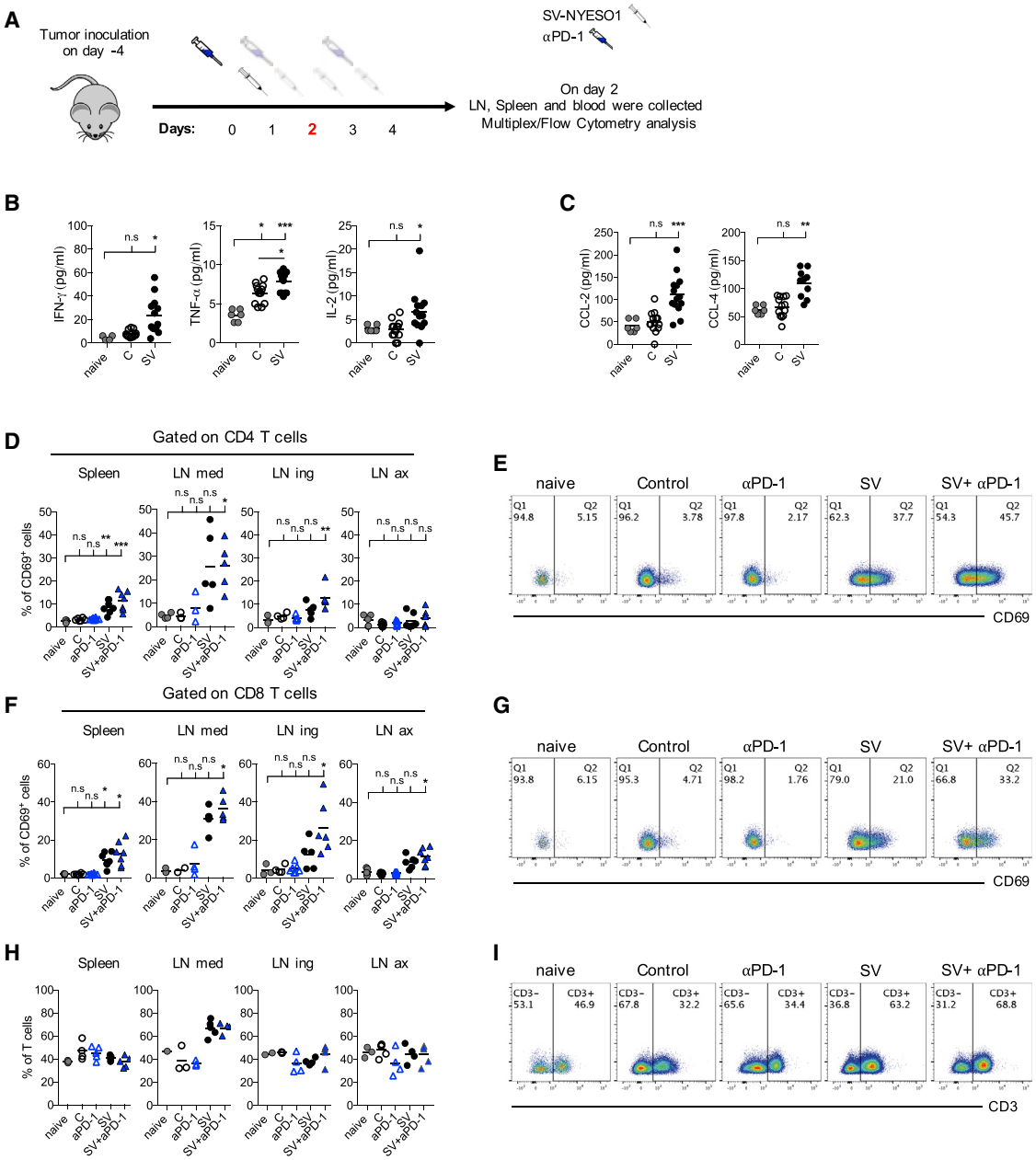

Figure 3. SV-NYESO1 Acts as an Immunostimulatory Agent and Induces a Rapid and Systemic T Cell Activation in Peripheral Lymphoid Organs

(A) Treatment schema. Tumor-bearing mice were left untreated or were treated with one injection of anti-PD-1 and/or SV-NYESO1. On day 2, organs and blood were collected from mice for flow cytometry and multiplex analysis, respectively. (B and C) Plasma samples from naive, control, and SV-NYESO1-treated mice were collected on day 2. Cytokine (B) and chemokine (C) levels in plasma samples were determined by multiplex assay. (E, G, and I) Representative flow cytometry plots of the mediastinal lymph node. (D–G) Percentage of CD69 expression by $CD4^+$ T cells (D and E) and $CD8^+$ T cells (F and G). Left to right, spleen, mediastinal (LN med), inguinal (LN ing), and axillary lymph nodes (LN ax). (H and I) T cell frequency was analyzed in naive mice and control or treated tumor-bearing mice. Results are representatives from two independent experiments. (B–I) Lines represent means, and statistical significance was determined with the Kurskal-Wallis test followed by the Dunns' test and with the Mann-Whitney test (B). n.s. > 0.05, *$p < 0.05$, **$p \leq 0.01$, ***$p \leq 0.001$.

correlates with the tumor cell viability. Viability of CT26.NYESO1 was markedly reduced at both E/T ratios (10:1 and 50:1) when co-cultured with splenocytes from mice receiving combined therapy compared with splenocytes from naive, control, and mice treated with anti-PD-1 alone. The cytotoxic potential of splenocytes from mice treated with SV-NYESO1 alone was weaker than that from

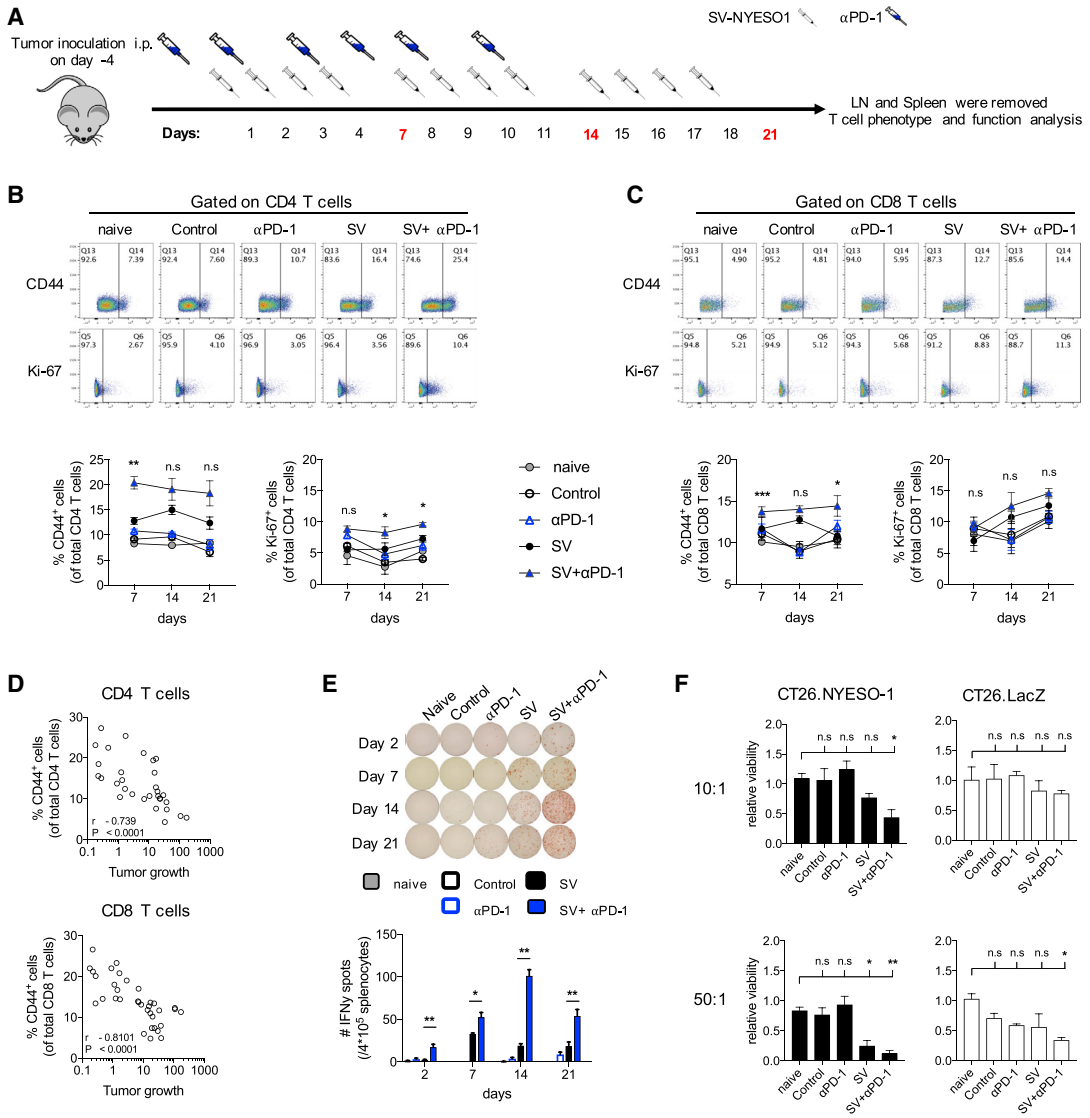

Figure 4. The Presence of Anti-PD-1 Antibody Enhances T Cell Activation and Function during SV-NYESO1 Therapy

(A) Treatment schema. Tumor-bearing mice were left untreated or were treated with SV with or without anti-PD-1. Mice were sacrificed on day 7, 14, or 21 to analyze the T cell immune response in spleen. (B and C) Percentage of CD44 and Ki-67 expression by $CD4^+$ T cells (B) and $CD8^+$ T cells (C) in naive mice as well as control and treated tumor-bearing mice using flow cytometry (n = 8 mice per group). Top graphs, representative flow cytometry plots from day 14. Bottom graphs, symbols summarizing data from two independent experiments. Statistical significance between groups treated with SV in presence or absence of anti-PD-1 was determined with the Mann-Whitney test. (D) Correlation of splenic $CD4^+$ T cells or $CD8^+$ T cells CD44 expression against tumor growth on day 14 by the Spearman-rank correlation test. (E) Interferon-γ (IFN-γ) enzyme-linked immunospot analysis of splenocytes harvested on day 14 from control and treated mice (n = 8 mice per group). (F) Cytotoxic activity of splenocytes harvested on day 14 from control and treated mice (n = 5 mice per group). Splenocytes were co-cultured with either CT26.Fluc.NYESO1 (left column) or CT26.Fluc.LacZ (right column) at various ratios for 2 days. Cytotoxic activity was assessed based on the viability of CT26 cells, which was determined by measuring the luciferase activity and is shown relative to naive splenocytes. Results are representatives from two independent experiments. (B, C, E, and F) Bars or symbols represent means ± SEM, and statistical significance was determined with the Mann-Whitney test (B, C, and E) or with the Kurskal-Wallis test followed by the Dunns' test (F). n.s. > 0.05, *p < 0.05, **p ≤ 0.01, ***p ≤ 0.001.

combined therapy. Our results also indicate that cytotoxicity was TAA dependent, as the viability of CT26-expressing LacZ remained stable across all groups. Only splenocytes from combined therapy showed some killing potential toward CT26.LacZ at an E/T ratio of 50:1, suggesting that SV-NYESO1 in combination with anti-PD-1 may induce a broader immune response and favor epitope spreading.

Together, these results clearly show that the addition of anti-PD-1 to SV-NYESO1 therapy enhances T cell activation over the course

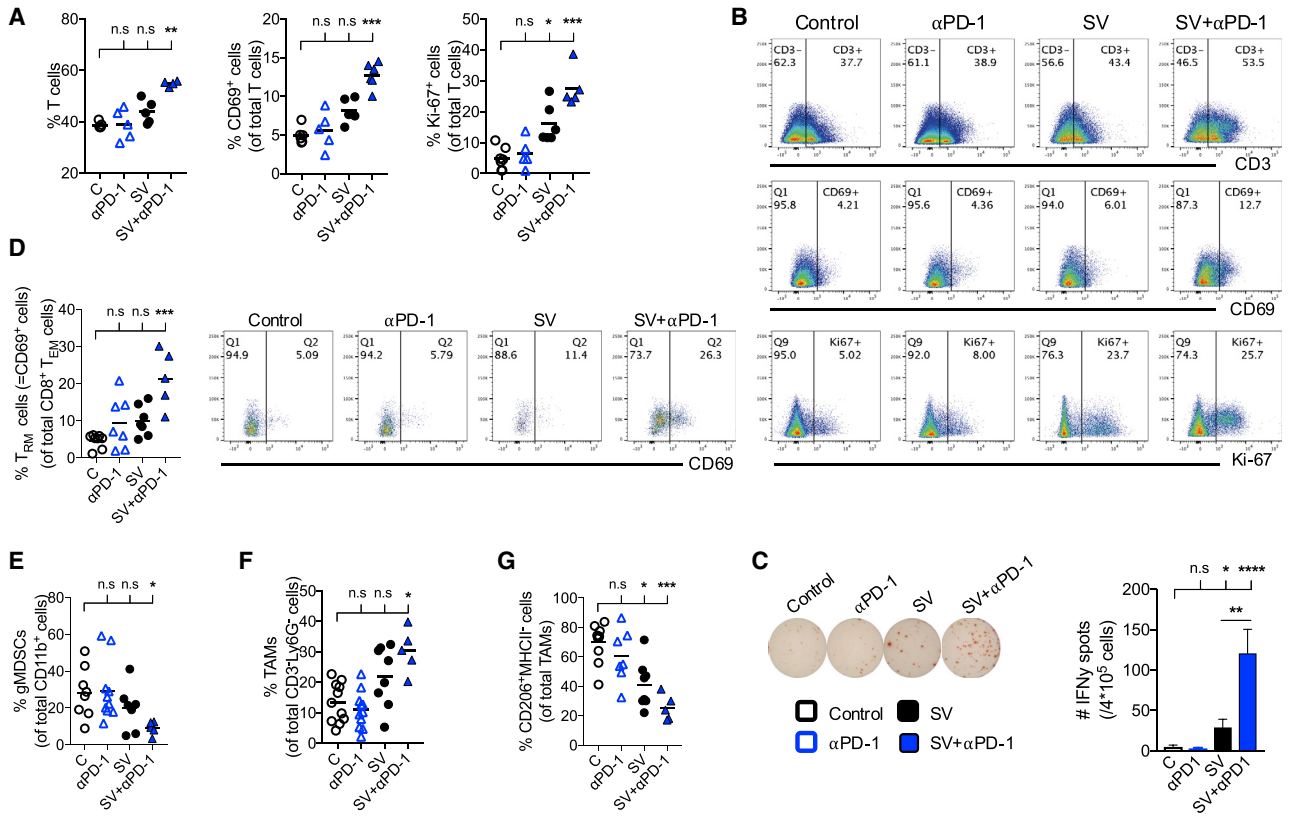

Figure 5. Mice Treated with SV-NYESO1 in Combination with Anti-PD-1 Display Enhanced Intratumoral T Cell Immunity

Tumors were harvested after 2 weeks of treatment from control and treated mice (n = 5–8 mice per group). (A and B) T cell immune response from indicated groups were assessed by flow cytometry. (A) Left graph, T cell frequency. Middle graph, percentage of CD69 expression by T cells. Right graph, percentage of Ki-67 expression by T cells. (B) Representative flow cytometry plots. (C) Interferon-γ (IFN-γ) enzyme-linked immunospot analysis of tumor-infiltrating cells from control and treated mice. (D) Resident-memory T cell frequency from indicated groups were assessed by flow cytometry and shown in dot plots and bar graph. (E–G) Frequencies of various myeloid cells in tumors from indicated groups were assessed by flow cytometry. (E) Granulocytic-myeloid-derived suppressor cell (gMDSC) frequency. (F) Tumor-associated macrophage (TAM) frequency. (G) Frequency of $CD206^{+}MHCII^{-}$ cell as a proportion of TAMs. Results are representatives from two independent experiments. Bars and lines represent means ± SEM, and statistical significance was determined with the Kurskal-Wallis test followed by the Dunns' test (A–G) or the Mann-Whitney test (C). n.s. > 0.05, *p < 0.05, **p ≤ 0.01, ***p ≤ 0.001, ****p ≤ 0.0001.

of treatment, which results in improved IFN-γ production and cytotoxic activity. In line with these results, a highly significant negative correlation between T cell activation and tumor growth was demonstrated, indicating a crucial role of T cells in controlling tumor growth. Thus, SV-NYESO1 acts as an initial stimulus to activate the immune response. The presence of anti-PD-1 helps to keep T cells activated and to further enhance T cell function.

Mice Treated with SV-NYESO1 in Combination with Anti-PD-1 Display Enhanced Intratumoral Immunity

Not only does SV-NYESO1 enter peripheral lymphoid organs and induce a systemic response, but like many other OVs, it can directly infect cancer cells and provide a local immune response in the tumor microenviroment.[11] However, as shown in previous publications, CT26 cells are not infected by SV *in vitro* or *in vivo*,[26,31] suggesting that the powerful therapeutic effect observed from combined therapy is not a direct result of tumor cell targeting. Thus, we wondered whether SV-NYESO1 therapy in combination with anti-PD-1 can nevertheless alter the local tumor microenvironment and favor an intratumoral immunity.

To assess the immune response in the tumor microenviroment, tumors were harvested from all groups after 2 weeks of treatment, and immune cells were analyzed by flow cytometry. A strong T cell infiltration was observed in animals treated with combined therapy (Figures 5A and 5B). Furthermore, T cell activation was markedly enhanced, as judged by CD69 and Ki-67 expression, in mice treated with SV-NYESO1 with anti-PD-1 when compared with naive mice as well as control and mice treated with anti-PD-1 alone. T cell activation was also observed in mice treated with SV-NYESO1 alone, although to a lesser extent. These results were reflected by the IFN-γ production from tumor infiltrating cells measured by ELISPOT (Figure 5C).

The presence of tissue-resident memory T cells (T_{RM}) in tumors has been linked with improved overall survival in both mice and humans.[32–34] Consistent with those results, a 4-fold increase in T_{RM} cells was detected in tumors from mice treated with combined therapy compared with naive mice (Figure 5D). The overall increase in intratumoral T cell response in mice treated with SV-NYESO1 and anti-PD-1 is also in accordance with a significant reduction of granulocytic myeloid-derived suppressor cells (gMDSC) and tumor-associated macrophages (TAMs) with a pro-tumor "M2" state (Figures 5E and 5G). Reduction of both cell types in tumors was also observed in mice treated with SV-NYESO1 alone, although to a lesser extent. Interestingly, an overall increase in TAMs was detected during SV-NYESO1 therapy (Figures 5F and S5). This indicates an increase in inflammatory "M1" like TAMs in tumors, which have been correlated with a reduction in tumor growth and prolonged survival time in humans and mice.[35,36]

Collectively, these findings reveal that SV-NYESO1 therapy produces a favorable intratumoral immune response with increased number of activated T cells and percentage of T_{RM} cells, as well as more inflammatory M1 TAMs and fewer suppressor cells, such as gMDSC and M2 TAMs. The addition of anti-PD-1 to SV-NYESO1 therapy strongly enhances these trends, inducing a better immune response within the tumor microenvironment.

Combined Therapy Favors the Formation of Effector Memory T Cells, Providing Long-Term Immunity against Recurrence

An important goal of successful anti-tumoral immunity is the development of long-term protective immunity to prevent relapse metastases and recurrences. To investigate whether SV-NYESO1 therapy induces T cell memory formation, the phenotype of T cells in all groups was investigated by flow cytometry in the spleen and tumor after 3 weeks of treatment (Figure 6). Splenocytes from untreated (control) mice and mice treated with anti-PD-1 alone demonstrated percentages of central-memory (T_{CM}) and effector-memory (T_{EM}) T cells similar to naive splenocytes, with 7% and 4%, respectively (Figure 6A). Treatment with SV-NYESO1 alone or in combination with anti-PD-1 showed a slight enhancement of T_{CM} (11% or 14%, respectively) but not of T_{EM} (4% and 6%, respectively). After 3 months, surviving mice that received combined therapy demonstrated enhanced formation of T_{EM} (19%) with a similar percentage of T_{CM} (10%). The same observations were made in tumors. Tumors treated with combined therapy induced 20% T_{EM}, while control and anti-PD-1- and SV-NYESO1-treated mice showed 5%, 7%, and 8%, respectively (Figure 6B). The percentage of T_{CM} remained stable in all groups.

To test whether enhanced T cell memory formation correlates with long-lived protection against the same cancer, we rechallenged mice after 200 days with CT26.Fluc.NYESO1 (Figures 6C, 6D, and S6). As epitope spreading was previously observed to occur during SV therapy,[26] mice were rechallenged with a closely related tumor lacking NYESO-1, CT26.Fluc.LacZ. Indeed, mice cured by combined therapy were immune to rechallenge with the same tumor as well as the closely related tumor. These results demonstrate that SV-NYESO1 in combination with anti-PD-1 enhances the formation of T_{EM} in the spleen and tumor, which provides long-term immunity against closely related cancer.

DISCUSSION

In this study, we show a potent therapeutic effect of SV expressing the TAA NYESO-1 in combination with anti-PD-1 in NYESO-1-expressing, tumor-bearing mice. Our data demonstrate a systemic lymphocyte activation and induction of pro-inflammatory cytokines and chemokines after a single SV-NYESO1 injection. In a model system where anti-PD-1 induces a moderate therapeutic effect, the introduction of SV leads to a curative result as well as protection against tumor relapses. Anti-PD-1 contributes to SV therapy by enhancing T cell activation, as judged by IFN-γ production and cytotoxic activity, in spleen and tumors during treatment. The role of T cell responses is clear in that an inverse correlation is seen between T cell activation and tumor growth. These findings account for total tumor clearance in mice treated with SV-NYESO1 and anti-PD-1. In short, SV-NYESO1 acts as an immunostimulatory agent inducing a strong systemic inflammatory response, while anti-PD-1 improves the magnitude of the anti-tumor T cell response in spleen and tumor.

Previous data from our lab demonstrated complete clearance of LacZ expressing tumors in mice treated with SV-LacZ alone.[26] The addition of an immune checkpoint blockade antibody was not needed. The reason of this discrepancy is not fully understood. However, the choice of TAA expressed by SV might play an important role. Granot et al. used the foreign antigen LacZ, which is expressed in *Escherichia coli*, as a TAA.[26] NYESO-1 is a human cancer testis antigen and has distant cousin in mice, ESO-3, which shares 42% identity with human NYESO-1. In addition, using different algorithms to detect potential epitopes in proteins demonstrated that LacZ expresses seven strong epitopes that bind to H2-K^d, whereas NYESO-1 expresses only one strong epitope on that major histocompatibility complex (MHC) molecule. The same trend was also observed for CD4 T cell epitopes presented by H2-IA^d. Thus, LacZ might be more immunogenic than NYESO-1 leading to a stronger and more diverse immune response. We demonstrated in this study that the therapeutic efficacy of the TAA expressed by SV also depends on the tumor model as SV-LacZ was unable to cure mice bearing CT26.NYESO1 tumors. This is most likely due to the fact that SV-LacZ induces a strong LacZ-specific T cell response, which cannot recognize the tumor anymore.[26] These observations indicate that the choice of TAA expressed by SV is crucial for an initial adequate antitumor immune response. Subsequently, a diversified T cell response develops that contributes to long-term protection.[26]

Treatment with anti-PD-1 or anti-PD-L1 antibodies results in long-lasting antitumor responses in patients with various cancers.[37–40] However, only a subset of patients respond to therapy, and it was previously observed that patients who did not respond to treatment were more likely to lack $CD8^+$ T cells inside tumors;[6,41] if no $CD8^+$ T cells are present that can be inhibited by PD-1:PD-L1 interaction, then

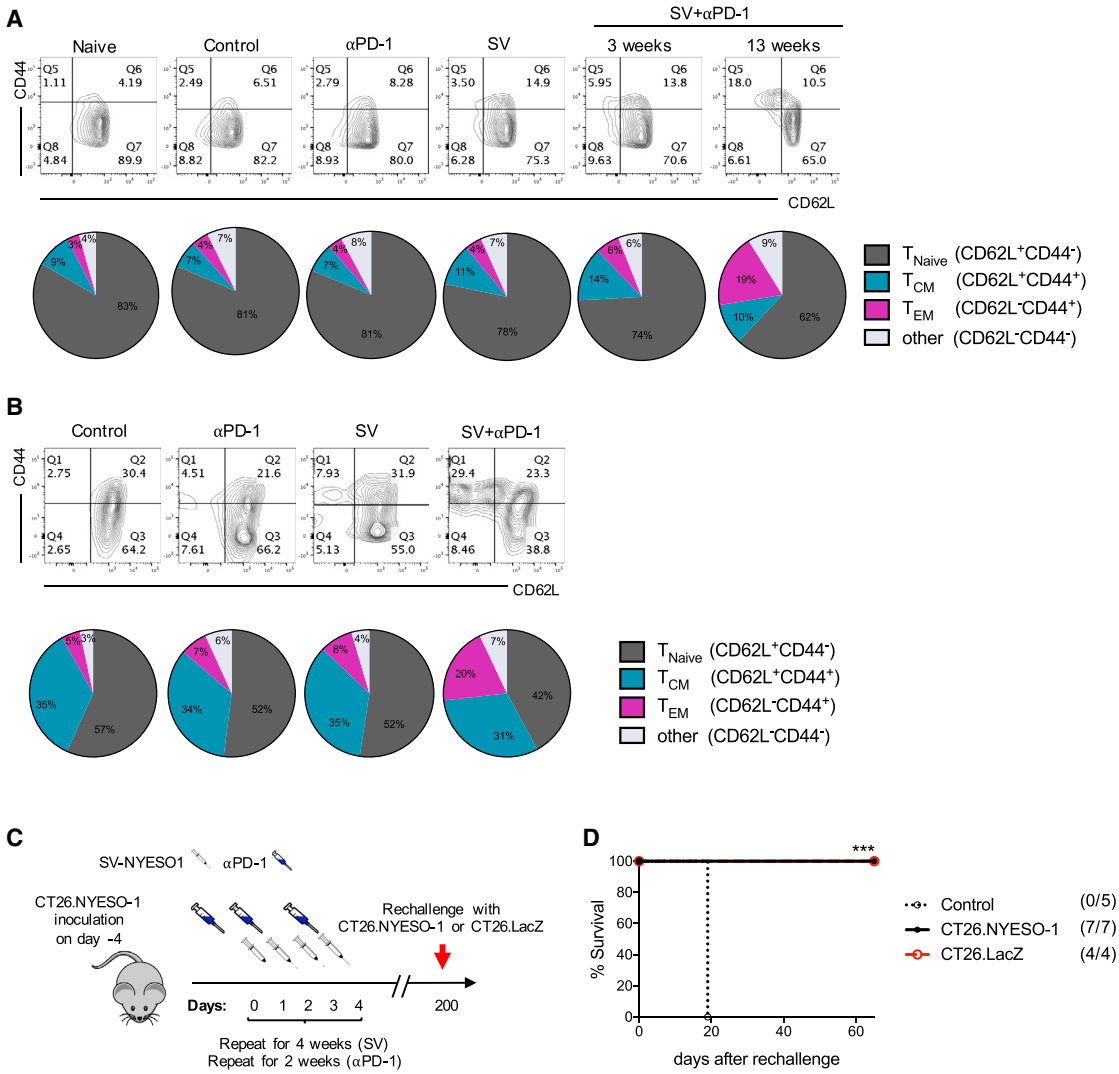

Figure 6. Memory T Cells Are Enriched in Spleen and Tumor of Mice Treated with SV-NYESO1 in Combination with Anti-PD-1, Providing Long-Term Immunity against Closely Related Tumors

(A and B) Memory phenotype of T cells was characterized in spleen and tumor from indicated groups by flow cytometry by gating on $CD3^+$ cells. The percentage of T cells expressing CD62L and/or CD44 was analyzed and shown as contour plots and pie charts, summarizing data from two independent experiments. (A) Splenocytes were harvested 3 and 13 weeks after the beginning of treatment from indicated groups (n = 8 mice per group). (B) Tumors were harvested 3 weeks after the beginning of treatment from indicated groups (n = 5–8 mice per group). (C) Treatment schema. Tumor-cured mice after SV therapy were rechallenged with the same cancer CT26.Fluc.NYESO1 at more than 150 days after the last SV treatment, and tumor growth was analyzed every day by noninvasive bioluminescent imaging. (D) Survival plots of naive (control, n = 5) and tumor-cured mice (n = 11) after rechallenge with CT26.Fluc.NYESO1 (n = 7) or CT26.Fluc.LacZ (n = 4). Statistical significance between tumor-cured and control (naive) mice was determined with the Mantel-Cox text. n.s. > 0.05, ***$p \leq 0.001$.

PD-1 blockade therapy is unlikely to work as well.[42–44] Another reason why patients might not respond to PD-1 blockade therapy is the low expression of PD-L1 and PD-1 on tumor cells and tumor-infiltrating T cells, respectively.[6,9,45,46] PD-L1 expression on tumor cells is induced by IFN-γ, a mechanism that appears to have evolved to evade destruction by the immune system.[42,44] Here, we show that SV-NYESO1 therapy increases T cell infiltration in tumors as well as enhances IFN-γ production by tumor-infiltrating lymphocytes. In addition, SV-NYESO1 induces PD-L1 and PD-1 expression on tumor cells and on tumor-infiltrating T cells, respectively. The mechanism behind PD-L1 induction during SV therapy is likely due to increased presence of activated tumor-infiltrating cells, such as T and NK cells, resulting in higher IFN-γ levels rather than an immediate-early response to type I IFN in the tumor microenvironment as demonstrated by Zamarin et al.[47] Due to increased PD-1 and PD-L1 expression in the tumor microenvironment, it is reasonable to suggest that

antitumor immune responses initiated by SV infection could be enhanced by combination with immune checkpoint therapy. Indeed, T cell response in the spleen and tumors was strongly enhanced in presence of the immune checkpoint blockade anti-PD-1. Our findings are in line with several other mouse studies using various OVs, such as Newcastle disease virus,[13,47] Maraba virus,[15] and Reovirus.[16,48] Results from a phase 1b trial in humans investigating the use of T-Vec in combination with anti-PD-1 support the findings in murine models.[9]

We show that SV-NYESO1 therapy leads to long-term protection against recurrences of the originally seeded tumor, indicating both a therapeutic and prophylactic effect of SV-NYESO1. This observation is in line with enhanced formation of T_{EM} cells in the spleen after treatment. Increased frequency of T_{EM} and T_{RM} was also observed in tumors during combined therapy. T_{RM} cells are characterized by stable surface expression of CD69 and an enhanced effector ability that functionally provides a tissue-wide alert state against local reinfection.[49–51] These results coincide with previous studies in humans and mice showing a correlation between tumor infiltration of T cells with a T_{RM} cell-like phenotype and improved overall survival.[32–34,52,53] In murine studies, the presence of T_{RM} cells was also shown to improve the anti-tumor response and provide long-term immunity to cancer. Furthermore, anti-PD-1 treatment promotes the infiltration of T_{CM} cells that can differentiate into T_{RM} cells following viral infection.[53] Therefore, the combination of SV and anti-PD-1 is needed for increased T_{RM} presence in tumors.

Tumor-cured mice after SV-NYESO1 treatment were also protected against a closely related tumor lacking the TAA NYESO-1, CT26.LacZ. In line with these results, we showed that splenocytes from combined therapy-treated mice exhibited cytotoxicity against not only CT26.NYESO1 cells but also CT26.LacZ. These results suggest that an immune response to endogenous CT26 tumor antigens developed as a consequence of SV-NYESO1 therapy, a concept known as epitope spreading.[54]

Most OVs are administrated intratumorally, which limits the possibility of cancer treatment to easily accessible ones, such as melanoma.[9,13,14] We show that i.p. injections of SV-NYESO1 induces an intratumoral immune response and changes the tumor microenvironment by promoting T cell recruitment and activation as well as deflection of M2 to M1 macrophages in tumors. Our findings are in line with those obtained by Samson et al.[16] and Bourgeois-Daigneault et al.,[15] where they show that intravenous infusion of OVs are effective in generating an anti-tumor immunity. Interestingly, in our tumor model, SV does not directly infect tumor cells, indicating that the therapeutic effect observed in tumors during treatment is not a direct result of tumor cell targeting. Rather, SV quickly localizes in LNs—infecting monocytes and macrophages—where T cells are primed against the TAA expressed by SV.[26,55,56] The recruitment of T cells to the mediastinal LN on day 2, as well as the increased T cell activation compared with spleen and other LNs, are indications that SV is inducing a T cell response in the mediastinal LN. One particular advantage of alphaviruses is that they are known to target LNs.[57] We propose that this is a strong advantage of SV, as TAAs can be directly delivered to LNs, enabling more efficient and quicker T cell priming.

Ovarian cancer ranks fifth in cancer deaths among women due to the fact that the majority of patients are diagnosed at a late disease stage and in most cases total cytoreductive surgery may not be technically fully possible anymore.[58] Thus, there is an urgent need for new therapeutic approaches for ovarian cancer. The use of SV-NYESO1 is attractive for several reasons. One is that approximately 43% of ovarian cancer cases express NYESO-1,[27] and SVs have been shown, once they trigger an antigen-specific T cell response, to subsequently induce a diversified T cell response that can recognize additional TAAs present in the tumor.[26] In addition, one of the challenges during single-agent immunotherapy with checkpoint inhibitors in ovarian cancer treatment has been that the number of tumor-infiltrating lymphocytes and the number of cells that express PD-L1 are both relatively low.[59]

We demonstrate here that SVNYESO-1 and anti-PD-1 have the potential to overcome these limitations and are very effective in murine models of ovarian cancer.[60,61] Furthermore, the fact that SV-NYESO1 treatment can be administrated i.p. or intravenously rather than intratumorally is an additional advantage that facilitates eliciting a strong cellular immune response. We expect that the premises and observations discussed in this study will help guide the clinical development of SV-NYESO1 therapy in an upcoming NIH-funded phase I dose-escalation study using this vector as an i.p. consolidation immunotherapy in women with residual or recurrent ovarian cancer status after chemotherapy.

MATERIALS AND METHODS

Study Design

The overall study was designed to investigate the therapeutic efficacy of SV-NYESO1 therapy with or without immune checkpoint blockade anti-PD-1 in mice bearing NYESO-1-expressing tumors. Further experiments were designed to evaluate the immune response to SV therapy. In all experiments, to ensure similar tumor sizes in all groups, mice were randomized only after tumors were established and before SV treatment (day 0). Tumor inoculated mice that showed a tumor signal below 10^5 relative luminescence units (RLU) before treatment were excluded from our study. The numbers of mice, statistical tests, and numbers of experimental replicates performed for each experiment are included in the figure legends. Data include all outliers, and investigators were not blinded during evaluation of the *in vivo* experiments.

Cell Lines

Baby hamster kidney (BHK), BALB/c colon carcinoma (CT26), and the CT26-expressing LacZ (CT26.LacZ) cell lines were obtained from the American Type Culture Collection (ATCC). Firefly luciferase (Fluc)-expressing CT26 cells (CT26.Fluc and CT26.LacZ.Fluc) were generated by stable transfection of pGL4.20_Fluc plasmid. The

CT26 cell line expressing both Fluc and NYESO-1 (CT26.Fluc.NYESO1) was generated by stably transfecting the CT26.Fluc cell line with the expression plasmid pReceiver-M02 (GeneCopoeia) that has NYESO-1 (NM_001327.1).

BHK cells were maintained in minimum essential α-modified media (α-MEM) (Corning CellGro) with 5% fetal bovine serum (FBS; Gibco) and 100 mg/mL penicillin-streptomycin (Corning CellGro). CT26.Fluc.NYESO1 and CT26.Fluc.LacZ cells were maintained in DMEM containing 4.5 g/L glucose (DMEM, Corning CellGro) supplemented with 10% FBS, 100 mg/mL penicillin-streptomycin, 7.5 μg/mL Puromycin, and 800 or 400 μg/mL Geneticin, respectively. All cell lines were cultured at 37°C and 5% CO_2.

SV Production

Sindbis replicon expressing NYESO-1 cDNA (SV-NYESO1) was made by PCR amplification of the NYESO-1 gene from the pReceiver-M02 plasmid. Expression of the NYESO-1 gene was confirmed by western blot as described below for vector titering. Sindbis expressing the LacZ gene (SV-LacZ) has been described previously.[17]

Sindbis viral vectors expressing LacZ cDNA (SV-LacZ) or NYESO-1 (SV-NYESO1) were produced as previously described.[62] In brief, the DNA plasmids carrying the Sindbis replicon with the gene of interest or Sindbis helper sequences were linearized before *in vitro* transcription using the mMACHINE RNA transcription kit (Ambion, Austin, TX) following the manufacturer's protocol. Helper and replicon RNAs were mixed at a 1:1 ratio and were then electroporated into BHK cells. Media was replaced with OPTI-MEM (Invitrogen) and supplemented with 100 μg/mL $CaCl_2$. Supernatant was collected 24 hr later and stored at −80°C.

SV Quantification

Titers were determined making serial dilutions of the vector in Opti-mem-$CaCl_2$ and infecting BHK cells for an hour at room temperature (RT). Cells were washed with α-MEM media and incubated overnight (o/n) at 37°C and 5% CO_2. For SV-LacZ, we infected 10^4 BHK cells in 96-well plates with 50 μL/well and for SV-NYESO1, 10^5 BHK cells in 12-well plates with 250 uL/well. In both cases, protein extraction was performed using M-PER Mammalian Protein Extraction Reagent (Pierce). LacZ was detected using the All in One β-Gal Assay reagent kit (Pierce) following the manufacturer's protocol. NYESO-1 was detected by western blot following standard protocol, using as a primary antibody the anti-NYESO-1 clone E978 (Upstate) at a dilution 1/5,000 in Tris-buffered saline-Tween (TBS-T) with 5% non-fat milk. Vector titers refer to the number of infectious particles (transducing units per milliliter of supernatant [TU/mL]) and were estimated as the last dilution having detectable reporter activity.

Because different detection sensitivities are obtained by the β-gal assay and NYESO-1 western blot, vectors were also titered by RT-PCR on total RNA of infected BHK cells (Table S1). Both vectors were used at RT-PCR titer of 10^7–10^8 TU/mL, equivalent to 10^4–10^5 TU/mL NYESO1 western blot or 10^6–10^7 TU/mL β-gal assay.

In Vivo Experiments and Tumor Models

All experiments were performed in accordance with the Institute of Animal Care and Use Committee at New York University Health. Six- to twelve-week-old female BALB/c mice were purchased from Taconic (Germantown, NY). For the tumor model, 7×10^4 CT26.Fluc.NYESO1 cells in 500 μL OPTI-MEM were injected i.p. into the right side of the animal on day −4. For treatments, the virus (10^7–10^8 TU/mL) in a total volume of 500 μL was injected i.p. into the left side of the animal 4 days a week (days 1, 2, 3, and 4) for a total of 4 weeks. The immune checkpoint inhibitor anti-PD-1 (clone RMPI-14, BioXCell) was injected i.p. into the left side of the animal at a dose of 250 μg per injection. Anti-PD-1 was administrated 3 days a week (days 0, 2, and 4) for a total of 2 weeks. For the tumor rechallenge model, 7×10^4 CT26.Fluc.NYESO1 cells or 5×10^4 CT26.Fluc.LacZ cells were injected i.p. into the left side of the animal. Therapeutic efficacy of the treatment was monitored in two ways: tumor luminescence and survival. Noninvasive bioluminescent imaging was done using the IVIS Spectrum imaging system (Caliper Life Science), and tumor growth was quantified using the Living Image 3.0 software (Caliper Life Science) as previously described.[18] Relative tumor growth for each mouse was calculated dividing total body counts of a given day by total body counts of the first IVIS image. Survival was monitored and recorded daily.

Flow Cytometry

For flow cytometry analysis, spleens, LNs, and tumors were harvested from mice. The extracted LNs and tumors were chopped into small pieces and incubated with a digestive mix containing RPMI with collagenase IV (50 μg/mL) and DNaseI (20 U/mL) for 1 hr at 37°C. Tumor samples had additional hyaluronidase V (50 μg/mL) in the digestive mix.

Spleens, digested tumors, and LNs were mashed through a 70 μm strainer before red blood cells were lysed using ammonium-chloride-potassium (ACK) lysis (Gibco). Cells were washed with PBS containing 1% FBS, and surface receptors were stained using various antibodies (Table S2). Stained cells were then fixed with PBS containing 4% formaldehyde. For intracellular staining (Table S3), the forkhead box P3 (FOXP3) staining buffer set was used (eBioscience). Flow cytometry analysis was performed on a LSR II machine (BD Bioscience) and data were analyzed using FlowJo (Tree Star).

Enzyme-Linked Immunospot

Splenocytes were isolated as described for flow cytometry. To isolate tumor-infiltrating cells, digested tumors were mashed through a 70-μm strainer and incubated for 4 hr at 37°C until most tumor cells adhered to the flask. Floating cells were collected and used to characterize tumor-infiltrating cells. Splenocytes and tumor-infiltrating cells were prepared at various time points during treatment, and mouse IFN-γ ELISPOT was performed according to the manufacturer's protocol (BD Biosciences). 4×10^5 cells were plated per well o/n in RPMI supplemented with 10% FBS and stimulated with NYESO-1 peptide (RGPESRLLE) at a final concentration of 5 μg/mL.

Ex Vivo Cytotoxic Assay

Splenocytes were collected 14 days after treatment started. Splenocytes (4×10^6/mL) were co-cultured with CT26.Fluc.NYESO1 (2×10^4/mL) or CT26.Fluc.LacZ (2×10^4/mL) in a 24-well plate for 2 days in 1 mL RPMI supplemented with 10% FBS. Cells were washed with PBS and lysed with 100 μL of M-PER Mammalian Protein Extraction Reagent (Pierce) per well. Cytotoxicity was assessed based on the viability of CT26 cells, which was determined by measuring the luciferase activity in each well. Luciferase activity was measured by adding 100 μL of Steady-Glo reagent (Promega) to each cell lysate and measuring the luminescence using a GLOMAX portable luminometer (Promega).

Statistical Analysis

All statistical analyses were performed using GraphPad Prism 6.0 as described in the figure legends. Data are means ± SEM.

SUPPLEMENTAL INFORMATION

Supplemental Information includes six figures and three tables and can be found with this article online at https://doi.org/10.1016/j.omto.2018.04.004.

AUTHOR CONTRIBUTIONS

Study Design, I.S., A.H., D.M.; Experiment Design and Implementation, I.S., A.H., D.M., C.M.P., S.V.; Data Analysis, I.S., A.H.; Manuscript Preparation, I.S., A.H., D.M., C.P.; Writing – Review and Editing: I.S., D.M.; Funding Acquisition, D.M.

CONFLICTS OF INTEREST

All authors are employed by NYU Langone School of Medicine and have no employment relationship or consultancy agreement with Cynvec. I.S., A.H., C.P., and D.M. are inventors on one or several issued patents and/or patent applications held by NYU that cover Sindbis treatment of neoplasia. As part of the Research and Licensing agreement, authors who are inventors on patents are entitled to a portion of NYU Langone's royalties received from Cynvec, should Sindbis vectors be approved by the FDA for the treatment of cancer. As part of the Licensing agreement, NYU Langone has apportioned stock to D.M. from its equity stake equity in Cynvec. S.V. and C.M.P. declare that they have no competing interests.

ACKNOWLEDGMENTS

The authors are grateful to Dr. Silvana Opp and Dr. Minjun Yu for their careful reviewing of the manuscript. Funding was provided by NIH grant 5R44CA206606 and through a Research and Licensing Agreement between NYU Langone and Cynvec, which licenses the Sindbis technology to Cynvec.

REFERENCES

1. Wolchok, J.D., Chiarion-Sileni, V., Gonzalez, R., Rutkowski, P., Grob, J.J., Cowey, C.L., Lao, C.D., Wagstaff, J., Schadendorf, D., Ferrucci, P.F., et al. (2017). Overall survival with combined nivolumab and ipilimumab in advanced melanoma. N. Engl. J. Med. *377*, 1345–1356.

2. Pettitt, D., Arshad, Z., Smith, J., Stanic, T., Holländer, G., and Brindley, D. (2018). CAR-T cells: a systematic review and mixed methods analysis of the clinical trial landscape. Mol. Ther. *26*, 342–353.

3. Kenter, G.G., Welters, M.J., Valentijn, A.R., Lowik, M.J., Berends-van der Meer, D.M., Vloon, A.P., Essahsah, F., Fathers, L.M., Offringa, R., Drijfhout, J.W., et al. (2009). Vaccination against HPV-16 oncoproteins for vulvar intraepithelial neoplasia. N. Engl. J. Med. *361*, 1838–1847.

4. Massari, F., Di Nunno, V., Cubelli, M., Santoni, M., Fiorentino, M., Montironi, R., Cheng, L., Lopez-Beltran, A., Battelli, N., and Ardizzoni, A. (2018). Immune checkpoint inhibitors for metastatic bladder cancer. Cancer Treat. Rev. *64*, 11–20.

5. Sharma, P., Hu-Lieskovan, S., Wargo, J.A., and Ribas, A. (2017). Primary, adaptive, and acquired resistance to cancer immunotherapy. Cell *168*, 707–723.

6. Tumeh, P.C., Harview, C.L., Yearley, J.H., Shintaku, I.P., Taylor, E.J., Robert, L., Chmielowski, B., Spasic, M., Henry, G., Ciobanu, V., et al. (2014). PD-1 blockade induces responses by inhibiting adaptive immune resistance. Nature *515*, 568–571.

7. Andtbacka, R.H., Kaufman, H.L., Collichio, F., Amatruda, T., Senzer, N., Chesney, J., Delman, K.A., Spitler, L.E., Puzanov, I., Agarwala, S.S., et al. (2015). Talimogene laherparepvec improves durable response rate in patients with advanced melanoma. J. Clin. Oncol. *33*, 2780–2788.

8. Lawler, S.E., Speranza, M.C., Cho, C.F., and Chiocca, E.A. (2017). Oncolytic viruses in cancer treatment: a review. JAMA Oncol. *3*, 841–849.

9. Ribas, A., Dummer, R., Puzanov, I., VanderWalde, A., Andtbacka, R.H.I., Michielin, O., Olszanski, A.J., Malvehy, J., Cebon, J., Fernandez, E., et al. (2017). Oncolytic virotherapy promotes intratumoral T cell infiltration and improves anti-PD-1 immunotherapy. Cell *170*, 1109–1119.e10, e1110.

10. Patel, M.R., and Kratzke, R.A. (2013). Oncolytic virus therapy for cancer: the first wave of translational clinical trials. Transl. Res. *161*, 355–364.

11. Kaufman, H.L., Kohlhapp, F.J., and Zloza, A. (2015). Oncolytic viruses: a new class of immunotherapy drugs. Nat. Rev. Drug Discov. *14*, 642–662.

12. Guo, Z.S., and Bartlett, D.L. (2017). Editorial of the special issue: oncolytic viruses as a novel form of immunotherapy for cancer. Biomedicines *5*, 52.

13. Zamarin, D., Holmgaard, R.B., Subudhi, S.K., Park, J.S., Mansour, M., Palese, P., Merghoub, T., Wolchok, J.D., and Allison, J.P. (2014). Localized oncolytic virotherapy overcomes systemic tumor resistance to immune checkpoint blockade immunotherapy. Sci. Transl. Med. *6*, 226ra32.

14. Moesta, A.K., Cooke, K., Piasecki, J., Mitchell, P., Rottman, J.B., Fitzgerald, K., Zhan, J., Yang, B., Le, T., Belmontes, B., et al. (2017). Local delivery of OncoVEX$^{mGM\text{-}CSF}$ generates systemic antitumor immune responses enhanced by cytotoxic T-lymphocyte-associated protein blockade. Clin. Cancer Res. *23*, 6190–6202.

15. Bourgeois-Daigneault, M.C., Roy, D.G., Aitken, A.S., El Sayes, N., Martin, N.T., Varette, O., Falls, T., St-Germain, L.E., Pelin, A., Lichty, B.D., et al. (2018). Neoadjuvant oncolytic virotherapy before surgery sensitizes triple-negative breast cancer to immune checkpoint therapy. Sci. Transl. Med. *10*, eaao1641.

16. Samson, A., Scott, K.J., Taggart, D., West, E.J., Wilson, E., Nuovo, G.J., Thomson, S., Corns, R., Mathew, R.K., Fuller, M.J., et al. (2018). Intravenous delivery of oncolytic reovirus to brain tumor patients immunologically primes for subsequent checkpoint blockade. Sci. Transl. Med. *10*, eaam7577.

17. Tseng, J.C., Levin, B., Hirano, T., Yee, H., Pampeno, C., and Meruelo, D. (2002). In vivo antitumor activity of Sindbis viral vectors. J. Natl. Cancer Inst. *94*, 1790–1802.

18. Tseng, J.C., Levin, B., Hurtado, A., Yee, H., Perez de Castro, I., Jimenez, M., Shamamian, P., Jin, R., Novick, R.P., Pellicer, A., and Meruelo, D. (2004). Systemic tumor targeting and killing by Sindbis viral vectors. Nat. Biotechnol. *22*, 70–77.

19. Strauss, J.H., Wang, K.S., Schmaljohn, A.L., Kuhn, R.J., and Strauss, E.G. (1994). Host-cell receptors for Sindbis virus. Arch. Virol. Suppl. *9*, 473–484.

20. Hardwick, J.M., and Levine, B. (2000). Sindbis virus vector system for functional analysis of apoptosis regulators. Methods Enzymol. *322*, 492–508.

21. Brummer-Korvenkontio, M., Vapalahti, O., Kuusisto, P., Saikku, P., Manni, T., Koskela, P., Nygren, T., Brummer-Korvenkontio, H., and Vaheri, A. (2002). Epidemiology of Sindbis virus infections in Finland 1981-96: possible factors explaining a peculiar disease pattern. Epidemiol. Infect. *129*, 335–345.

22. Manni, T., Kurkela, S., Vaheri, A., and Vapalahti, O. (2008). Diagnostics of Pogosta disease: antigenic properties and evaluation of Sindbis virus IgM and IgG enzyme immunoassays. Vector Borne Zoonotic Dis. *8*, 303–311.

23. Sane, J., Kurkela, S., Lokki, M.L., Miettinen, A., Helve, T., Vaheri, A., and Vapalahti, O. (2012). Clinical Sindbis alphavirus infection is associated with HLA-DRB1*01 allele and production of autoantibodies. Clin. Infect. Dis. *55*, 358–363.

24. Sane, J. (2012). Sindbis virus as a human pathogen: epidemiology, virology, genetic susceptibility and pathogenesis. PhD thesis (Helsinki: University of Helsinki).

25. Bredenbeek, P.J., Frolov, I., Rice, C.M., and Schlesinger, S. (1993). Sindbis virus expression vectors: packaging of RNA replicons by using defective helper RNAs. J. Virol. *67*, 6439–6446.

26. Granot, T., Yamanashi, Y., and Meruelo, D. (2014). Sindbis viral vectors transiently deliver tumor-associated antigens to lymph nodes and elicit diversified antitumor $CD8^+$ T-cell immunity. Mol. Ther. *22*, 112–122.

27. Gnjatic, S., Nishikawa, H., Jungbluth, A.A., Güre, A.O., Ritter, G., Jäger, E., Knuth, A., Chen, Y.T., and Old, L.J. (2006). NY-ESO-1: review of an immunogenic tumor antigen. Adv. Cancer Res. *95*, 1–30.

28. Giavina-Bianchi, M., Giavina-Bianchi, P., Sotto, M.N., Muzikansky, A., Kalil, J., Festa-Neto, C., and Duncan, L.M. (2015). Increased NY-ESO-1 expression and reduced infiltrating $CD3^+$ T cells in cutaneous melanoma. J. Immunol. Res. *2015*, 761378.

29. Dong, Y., Sun, Q., and Zhang, X. (2017). PD-1 and its ligands are important immune checkpoints in cancer. Oncotarget *8*, 2171–2186.

30. Castellino, F., Huang, A.Y., Altan-Bonnet, G., Stoll, S., Scheinecker, C., and Germain, R.N. (2006). Chemokines enhance immunity by guiding naive $CD8^+$ T cells to sites of $CD4^+$ T cell-dendritic cell interaction. Nature *440*, 890–895.

31. Huang, P.Y., Guo, J.H., and Hwang, L.H. (2012). Oncolytic Sindbis virus targets tumors defective in the interferon response and induces significant bystander antitumor immunity in vivo. Mol. Ther. *20*, 298–305.

32. Malik, B.T., Byrne, K.T., Vella, J.L., Zhang, P., Shabaneh, T.B., Steinberg, S.M., Molodtsov, A.K., Bowers, J.S., Angeles, C.V., Paulos, C.M., et al. (2017). Resident memory T cells in the skin mediate durable immunity to melanoma. Sci. Immunol. *2*, https://doi.org/10.1126/sciimmunol.aam6346.

33. Webb, J.R., Milne, K., Watson, P., Deleeuw, R.J., and Nelson, B.H. (2014). Tumor-infiltrating lymphocytes expressing the tissue resident memory marker CD103 are associated with increased survival in high-grade serous ovarian cancer. Clin. Cancer Res. *20*, 434–444.

34. Djenidi, F., Adam, J., Goubar, A., Durgeau, A., Meurice, G., de Montpréville, V., Validire, P., Besse, B., and Mami-Chouaib, F. (2015). $CD8^+CD103^+$ tumor-infiltrating lymphocytes are tumor-specific tissue-resident memory T cells and a prognostic factor for survival in lung cancer patients. J. Immunol. *194*, 3475–3486.

35. Gordon, S.R., Maute, R.L., Dulken, B.W., Hutter, G., George, B.M., McCracken, M.N., Gupta, R., Tsai, J.M., Sinha, R., Corey, D., et al. (2017). PD-1 expression by tumour-associated macrophages inhibits phagocytosis and tumour immunity. Nature *545*, 495–499.

36. Ohri, C.M., Shikotra, A., Green, R.H., Waller, D.A., and Bradding, P. (2009). Macrophages within NSCLC tumour islets are predominantly of a cytotoxic M1 phenotype associated with extended survival. Eur. Respir. J. *33*, 118–126.

37. Sharma, P., and Allison, J.P. (2015). Immune checkpoint targeting in cancer therapy: toward combination strategies with curative potential. Cell *161*, 205–214.

38. Larkin, J., Chiarion-Sileni, V., Gonzalez, R., Grob, J.J., Cowey, C.L., Lao, C.D., Schadendorf, D., Dummer, R., Smylie, M., Rutkowski, P., et al. (2015). Combined Nivolumab and Ipilimumab or monotherapy in untreated melanoma. N. Engl. J. Med. *373*, 23–34.

39. Garon, E.B., Rizvi, N.A., Hui, R., Leighl, N., Balmanoukian, A.S., Eder, J.P., Patnaik, A., Aggarwal, C., Gubens, M., Horn, L., et al.; KEYNOTE-001 Investigators (2015). Pembrolizumab for the treatment of non-small-cell lung cancer. N. Engl. J. Med. *372*, 2018–2028.

40. Motzer, R.J., Rini, B.I., McDermott, D.F., Redman, B.G., Kuzel, T.M., Harrison, M.R., Vaishampayan, U.N., Drabkin, H.A., George, S., Logan, T.F., et al. (2015). Nivolumab for metastatic renal cell carcinoma: results of a randomized phase II trial. J. Clin. Oncol. *33*, 1430–1437.

41. Herbst, R.S., Soria, J.C., Kowanetz, M., Fine, G.D., Hamid, O., Gordon, M.S., Sosman, J.A., McDermott, D.F., Powderly, J.D., Gettinger, S.N., et al. (2014). Predictive correlates of response to the anti-PD-L1 antibody MPDL3280A in cancer patients. Nature *515*, 563–567.

42. Ribas, A. (2015). Adaptive immune resistance: how cancer protects from immune attack. Cancer Discov. *5*, 915–919.

43. Spranger, S., Spaapen, R.M., Zha, Y., Williams, J., Meng, Y., Ha, T.T., and Gajewski, T.F. (2013). Up-regulation of PD-L1, IDO, and T(regs) in the melanoma tumor microenvironment is driven by CD8(+) T cells. Sci. Transl. Med. *5*, 200ra116.

44. Pardoll, D.M. (2012). The blockade of immune checkpoints in cancer immunotherapy. Nat. Rev. Cancer *12*, 252–264.

45. Postow, M.A., Callahan, M.K., and Wolchok, J.D. (2015). Immune checkpoint blockade in cancer therapy. J. Clin. Oncol. *33*, 1974–1982.

46. Topalian, S.L., Hodi, F.S., Brahmer, J.R., Gettinger, S.N., Smith, D.C., McDermott, D.F., Powderly, J.D., Carvajal, R.D., Sosman, J.A., Atkins, M.B., et al. (2012). Safety, activity, and immune correlates of anti-PD-1 antibody in cancer. N. Engl. J. Med. *366*, 2443–2454.

47. Zamarin, D., Ricca, J.M., Sadekova, S., Oseledchyk, A., Yu, Y., Blumenschein, W.M., Wong, J., Gigoux, M., Merghoub, T., and Wolchok, J.D. (2018). PD-L1 in tumor microenvironment mediates resistance to oncolytic immunotherapy. J. Clin. Invest. *128*, 1413–1428.

48. Rajani, K., Parrish, C., Kottke, T., Thompson, J., Zaidi, S., Ilett, L., Shim, K.G., Diaz, R.M., Pandha, H., Harrington, K., et al. (2016). Combination therapy with reovirus and anti-PD-1 blockade controls tumor growth through innate and adaptive immune responses. Mol. Ther. *24*, 166–174.

49. Mueller, S.N., and Mackay, L.K. (2016). Tissue-resident memory T cells: local specialists in immune defence. Nat. Rev. Immunol. *16*, 79–89.

50. Clark, R.A. (2015). Resident memory T cells in human health and disease. Sci. Transl. Med. *7*, 269rv1.

51. Ariotti, S., Hogenbirk, M.A., Dijkgraaf, F.E., Visser, L.L., Hoekstra, M.E., Song, J.Y., Jacobs, H., Haanen, J.B., and Schumacher, T.N. (2014). T cell memory. Skin-resident memory $CD8^+$ T cells trigger a state of tissue-wide pathogen alert. Science *346*, 101–105.

52. Kho, J.Y., Gaspar, M.P., Kane, P.M., Jacoby, S.M., and Shin, E.K. (2017). Prognostic variables for patient return-to-work interval following carpal tunnel release in a workers' compensation population. Hand (N. Y.) *12*, 246–251.

53. Enamorado, M., Iborra, S., Priego, E., Cueto, F.J., Quintana, J.A., Martínez-Cano, S., Mejías-Pérez, E., Esteban, M., Melero, I., Hidalgo, A., and Sancho, D. (2017). Enhanced anti-tumour immunity requires the interplay between resident and circulating memory $CD8^+$ T cells. Nat. Commun. *8*, 16073.

54. Vanderlugt, C.L., and Miller, S.D. (2002). Epitope spreading in immune-mediated diseases: implications for immunotherapy. Nat. Rev. Immunol. *2*, 85–95.

55. Mokhtarian, F., Griffin, D.E., and Hirsch, R.L. (1982). Production of mononuclear cell chemotactic factors during Sindbis virus infection of mice. Infect. Immun. *35*, 965–973.

56. Assunção-Miranda, I., Bozza, M.T., and Da Poian, A.T. (2010). Pro-inflammatory response resulting from sindbis virus infection of human macrophages: implications for the pathogenesis of viral arthritis. J. Med. Virol. *82*, 164–174.

57. Choi, Y., and Chang, J. (2013). Viral vectors for vaccine applications. Clin. Exp. Vaccine Res. *2*, 97–105.

58. Oronsky, B., Ray, C.M., Spira, A.I., Trepel, J.B., Carter, C.A., and Cottrill, H.M. (2017). A brief review of the management of platinum-resistant-platinum-refractory ovarian cancer. Med. Oncol. *34*, 103.

59. Welch, A. (2018). Immunotherapy combinations on the horizon for ovarian cancer. Targeted Oncology. Published online January 9, 2018, http://www.targetedonc.com/news/immunotherapy-combinations-on-the-horizon-for-ovarian-cancer.

60. Tseng, J.C., Hurtado, A., Yee, H., Levin, B., Boivin, C., Benet, M., Blank, S.V., Pellicer, A., and Meruelo, D. (2004). Using sindbis viral vectors for specific detection and suppression of advanced ovarian cancer in animal models. Cancer Res. *64*, 6684–6692.

61. Unno, Y., Shino, Y., Kondo, F., Igarashi, N., Wang, G., Shimura, R., Yamaguchi, T., Asano, T., Saisho, H., Sekiya, S., and Shirasawa, H. (2005). Oncolytic viral therapy for cervical and ovarian cancer cells by Sindbis virus AR339 strain. Clin. Cancer Res. *11*, 4553–4560.

62. Hurtado, A., Tseng, J.C., Boivin, C., Levin, B., Yee, H., Pampeno, C., and Meruelo, D. (2005). Identification of amino acids of Sindbis virus E2 protein involved in targeting tumor metastases in vivo. Mol. Ther. *12*, 813–823.

OMTO, Volume *9*

Supplemental Information

Systemically Administered Sindbis Virus in Combination with Immune Checkpoint Blockade Induces Curative Anti-tumor Immunity

Iris Scherwitzl, Alicia Hurtado, Carolyn M. Pierce, Sandra Vogt, Christine Pampeno, and Daniel Meruelo

Supplementary Data

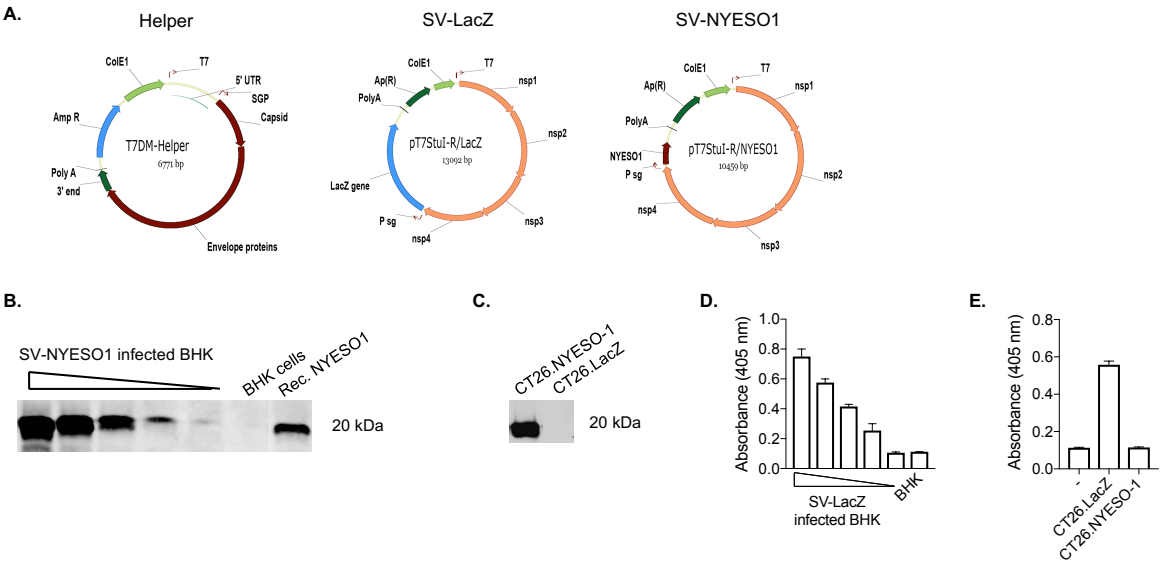

Supplemental Figure S1. Sindbis Virus can be genetically modified to express LacZ or NYESO-1.

A, Map of the helper replicon, SV-LacZ and SV-NYESO-1 plasmids. **B**, To verify NYESO-1 expression of SV-NYESO1, proteins were extracted from SV-NYESO1 infected BHK cells and NYESO-1 expression was detected by Western Blot. As a positive and negative control, recombinant NYESO-1 and uninfected BHK cells were used. **C**, NYESO-1 expression in CT26.Fluc.NYESO1 was verified by Western blot. CT26.Fluc.LacZ was used as a negative control **D**, To verify LacZ expression of SV-LacZ, Protein were extracted from SV-LacZ infected BHK cells and LacZ expression was detected using the mammalian β-Galactosidase assay kit. As a negative control, uninfected BHK cells were used. **E**, LacZ expression of the mouse colon carcinoma cell line CT26.Fluc.LacZ was verified using the mammalian β-Galactosidase assay kit. As a negative control, CT26.Fluc.NYESO1 cells were used.

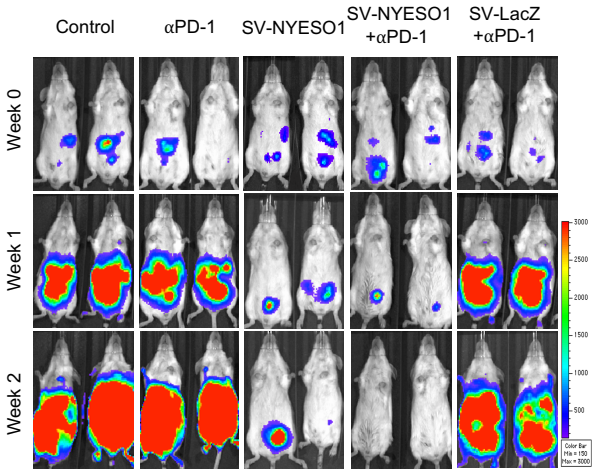

Supplemental Figure S2. Noninvasive bioluminescence images of CT26.Fluc.NYESO1 tumor bearing mice during SV treatment.

Representative bioluminescence images of three independent experiments showing control and treated mice bearing CT26.Fluc.NYESO1 tumors. Images were taken one day before starting SV treatment (day 0) and at weeks 1 and 2.

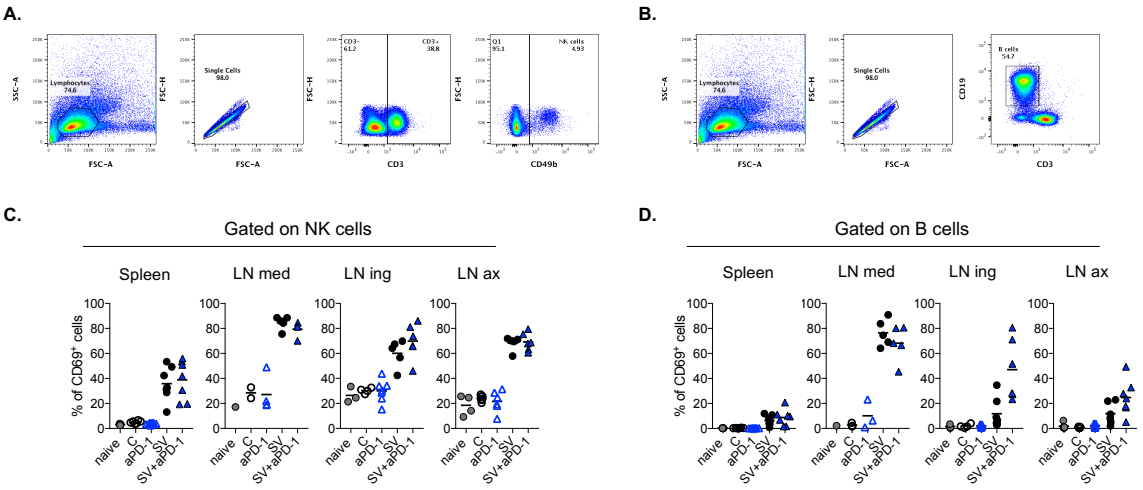

Supplemental Figure S3. SV-NYESO1 induces an early and systemic activation of NK and B cells.

CT26.Fluc.NYESO1 tumor cells were injected into BALB/c mice on day -4. One injection of anti-PD-1 (250 µg) and/or SV-NYESO1 was given to the respective groups on day 0 and 1, respectively. On day 2, mice were sacrificed and organs were removed and prepared for flow cytometry analysis. **A** and **B**, Flow cytometry gating strategy to define NK cells (A) and B cells (B). **C** and **D**, Percentage of CD69 expression by NK cells (C) and B cells (D). Left to right: spleen, mediastinal (LN med), inguinal (LN ing) and axillary lymph nodes (LN ax). Results are representatives from two independent experiments. Lines represent means and statistical significance was determined with the Kurskal-Wallis test followed by the Dunns' test.

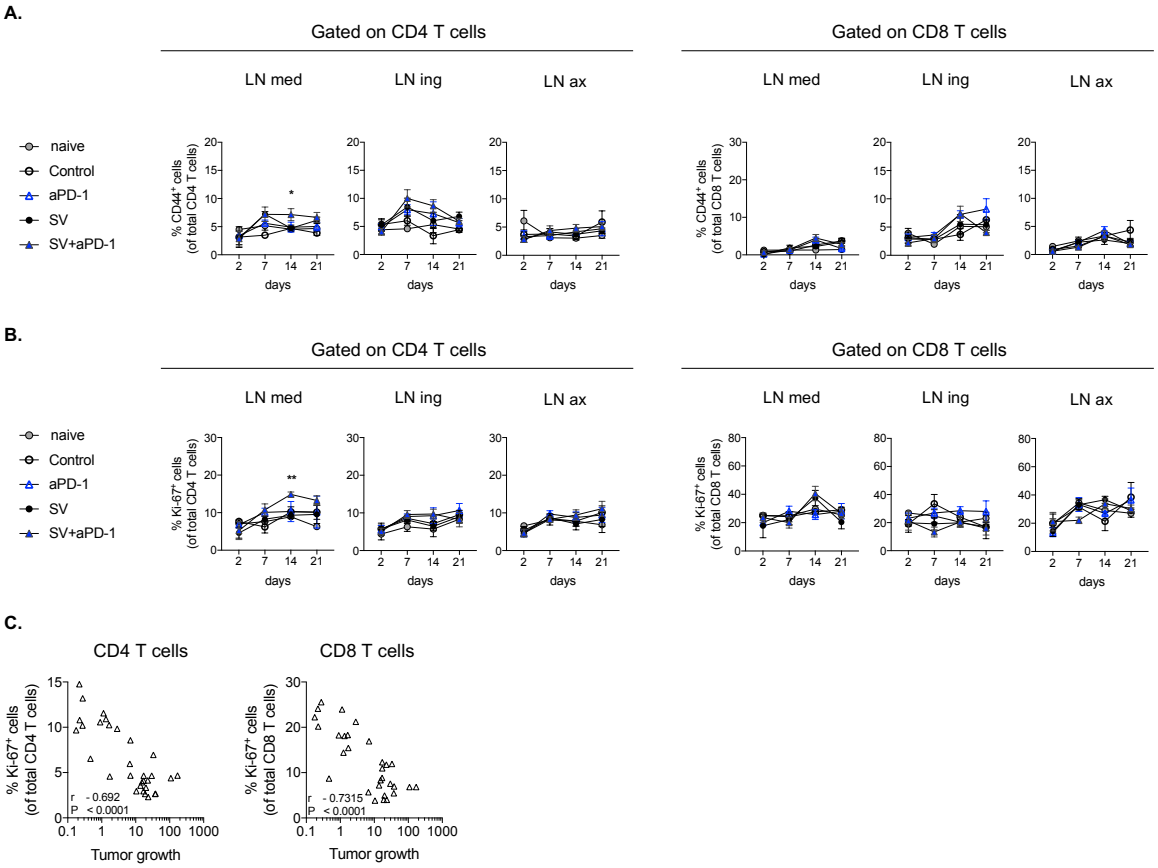

Supplemental Figure S4. T cell activation in peripheral lymphoid organs over the course of SV-NYESO1 treatment in presence or absence of anti-PD-1.

Tumor bearing BALB/c mice were left untreated or were treated with SV with or without anti-PD-1. Mice were sacrificed on day 2, 7, 14 or 21 to analyze the T cell immune response in spleen and mediastinal (med), inguinal (ing) and axillary (ax) lymph nodes (LN). **A** and **B**, Percentage of CD44 (A) and Ki-67 (B) expression by $CD4^+$ T cells and $CD8^+$ T cells in naive mice, as well as, control or treated tumor bearing mice using flow cytometry (n=8 mice per group). Left graphs: $CD4^+$ T cells. Right graphs: $CD8^+$ T cells. Symbols summarizing data from two independent experiments. Statistical significance between groups treated with SV in presence or absence of anti-PD-1 was determined with the Mann-Whitney test. **C**, Correlation of splenic

CD4$^+$ T cells or CD8$^+$ T cells Ki-67 expression against tumor growth on day 14 by the Spearman-rank correlation test. Results are representatives from two independent experiments. n.s > 0.05, $*P < 0.05$, $**P \leq 0.01$.

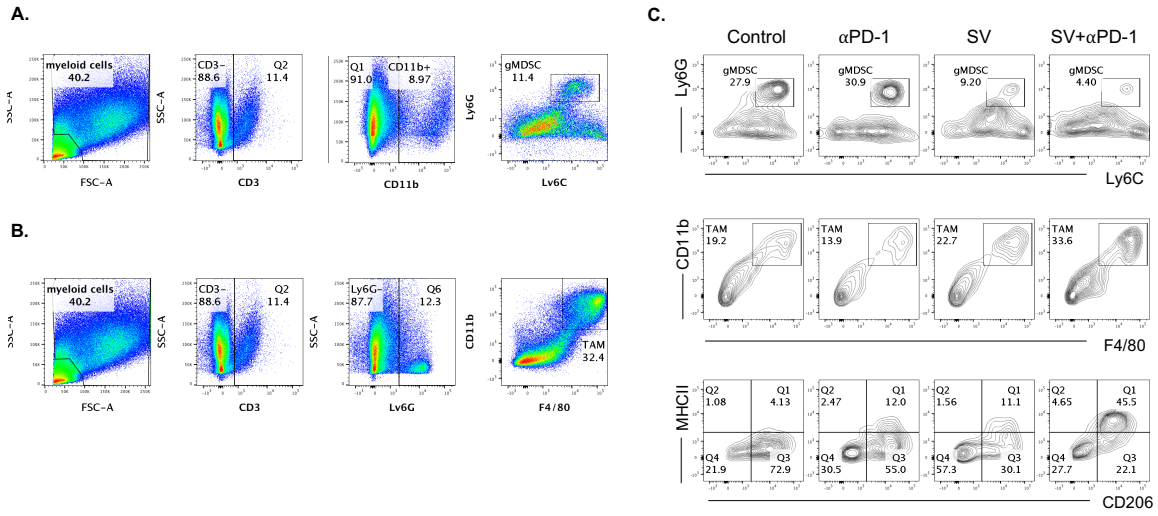

Supplemental Figure S5. Flow cytometry gating strategy for granulocytic-myeloid derived supressor cell and Tumor-associated macrophages in tumor.

A, Gating strategy of granulocytic-myeloid derived suppressor cells (gMDSC) by flow cytometry. **B**, Gating strategy of tumor-associated macrophages by flow cytometry. **C**, Representative flow cytometry plots of the frequencies of gMDSCs, TAMs and macrophage type 2 like cells from indicated groups.

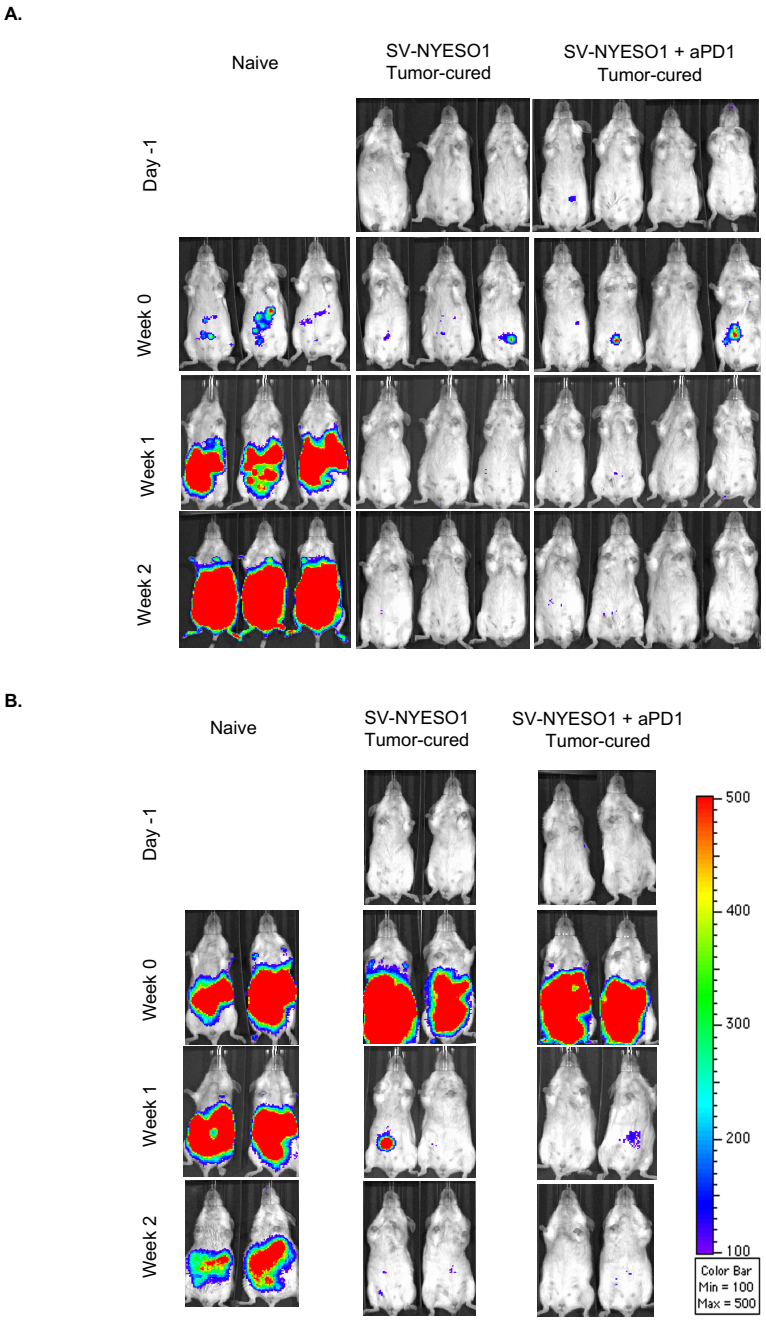

Supplemental Figure S6. Whole body bioluminescence images of rechallenged tumor cured mice.

Tumor cured mice were injected i.p. with 7 x 10^4 CT26.Fluc.NYESO1 cells (A; n=7) or 5 x 10^4 CT26.Fluc.LacZ cells (B; n=4) at 200 days after SV-NYESO1 or SV-NYESO1 with anti-PD-1

treatments. Bioluminescence was recorded one day before re-challenge for tumor cured mice as background signal control; one day after cells inoculation (Week 0) and then weekly. The scale used to prepare both figures is shown in (B).

Supplemental Table S1. Primers and conditions for RT-PCR used to titer vectors

cDNA (ThermoScript ™ RNaseH-reverse transcriptase (Invitrogen)		
primer	**Sequence**	**cDNA Cycle**
cDNA5R	5'- TTTTTGAAATGTTAAAAACAAAATTTTGTTG	2 hours at 60 °C
QPCR (IQ SYBR Green Supermix (BioRad))		
primer	**Sequence**	**cDNA Cycle**
7692F	5'-TGATCCGACCAGCAAAACTC	5 min at 95 °C 40 x [95 °C 20 sec; 60 °C 30 sec; 72 °C 30 sec]
cDNA5R	5'- TTTTTGAAATGTTAAAAACAAAATTTTGTTG	

Supplemental Table S2. FACS panel for surface markers.

Antibody	Clone	Fluorochrome	Vendor
CD3	17A2	BV786	Biolegend
CD3	17A2	BV605	Biolegend
CD4	RM4-4	PerCP-Cy5.5	Biolegend
CD8	53-6.7	APC-H7	BD Bioscience
CD11b	M1/70	BV786	Biolegend
CD11c	N418	PercP-Cy5.5	Biolegend
CD19	6D5	PE-Cy7	Biolegend
CD44	IM7	BV605	Biolegend
CD49b	DX5	PE	Biolegend
CD62L	MEL-14	Alexa Fluor 700	Biolegend
CD69	H1.2F3	FITC	Biolegend
Ly6C	HK1.4	PE-Cy7	Biolegend
Ly6G	1A8	BV421	Biolegend
PD-1	29F.1A12	APC	Biolegend
PD-L1	10F.9G2	PE	Biolegend
F4/80	T45-2342	PE-CF594	BD Bioscience
IA/IB	M5/114.15.2	V500	BD Bioscience

Supplemental Table S3. FACS panel for intracellular staining.

Antibody	Clone	Fluorochrome	Vendor
FoxP3	259D/C7	PE-CF594	BD Bioscience
Ki-67	16A8	BV421	Biolegend